6th International Meeting
on
Wind Turbine Noise
Glasgow 20-13 April 2015

Sound source localization on wind turbines using a single acoustic vector sensor.

Jasper Serraris. Microflown Technologies, Tivolilaan 205, 6824BV Arnhem, the Netherlands. E-mail: serraris@microflown.com

Daniel Fernández Comesaña. Microflown Technologies, Tivolilaan 205, 6824BV Arnhem, the Netherlands. E-mail: fernandez@microflown.com

Summary

In recent decades the use of wind turbines as important sources of sustainable energy has increased rapidly. Wind turbine manufacturers are constantly looking for opportunities to decrease the radiation of noise power, measured according to the IEC 61400-11 acoustic standard. Noise vibration and harshness engineers use sound visualization techniques as key tools in their effort to localize and reduce noise. A variety of sound visualization methods have been developed throughout history to improve the noise source information acquired. New developments enable the study of noise strength, location, radiation and distribution using visual approaches.

In this paper one application of a novel sound visualization technique is discussed. The method uses a single Acoustic Vector Sensor (AVS). The AVS consists of one pressure microphone and three orthogonally placed particle velocity sensors, spaced close together. The probe is positioned at a fixed location and beamforming algorithms are applied to define the origin of noise emissions. Short time requirements, high flexibility and low purchase costs make this method an efficient sound source visualization technique for stationary sound sources. This application concerns the initial investigation of a multi-megawatt wind turbine using a single AVS.

1. Introduction

Wind energy has become an important source of renewable energy for reducing carbon emission levels. The amount of wind turbines being built is increasing over time. Wind turbine manufacturers aim to design their wind turbines to radiate as low sound power levels as possible. In Europe, the radiation of the noise power produced by a wind turbine is measured according to the IEC 61400-11 standard. However, in this method the noise emission of the blades, generator and gears are all measured simultaneously.

Wind turbine manufacturers seek solutions to localize and rank noise sources. To determine the influence of separate components, several sound pressure based

methods are available. Among them, array beamforming is the most common method. It requires multiple pressure microphones and the amount of microphones increases as the frequency range and resolution of interest increases. To measure low frequencies, the sensors must be placed in an array that spans several meters in width and height.

In this paper a method for low frequency sound source localization on a multi-megawatt wind turbine is described. The method is based on measuring both sound pressure and particle velocity, using a single Acoustic Vector Sensor (AVS). The AVS used is the Microflown '3 Dimensional Sound Intensity Probe' (Figure 1) and comprises a sound pressure microphone and three closely spaced orthogonal particle velocity sensors. The AVS is used to provide the sound Direction of Arrival (DOA). The frequency band of interest will be called Frequency Band x (FBx) and falls within the 50 – 250 Hz range.

Preliminary research on sound source localization using a single AVS has been done over the last two decades, starting with the introduction of the signal model of a vector sensor into the field of signal processing by Nehorai and Paldi in 1994. Studies followed in which an AVS was used to localize a sound source in air (Raangs and Druyvesteyn, 2002) and distinguish two incoherent sound sources (Baste et al., 2009). Later, studies by Wind et al. (2009, 2010) and Jing (2014) reviewed the practical advantages of using an AVS over microphone arrays. Both studied different beamforming techniques such as the conventional Delay-And-Sum (DAS) beamforming and Minimum-Variance-Beamforming (MVB, also known as Capon).

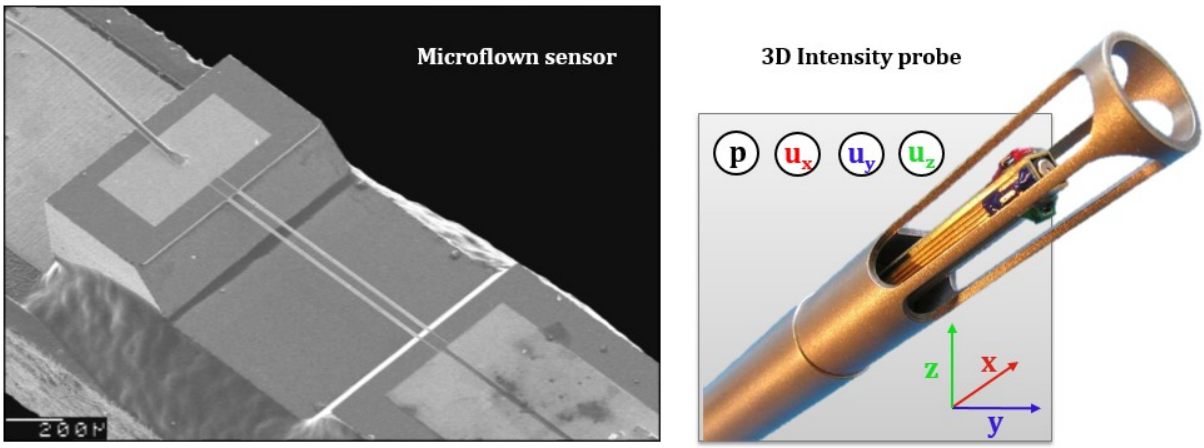

Figure 1: A single Microflown acoustic particle velocity sensor (left) and the 3 Dimensional Sound Intensity Probe (right.

2. Theory

Compared to traditional scalar sensor arrays comprising only sound pressure microphones, the Acoustic Vector Sensor (AVS) makes use of more available acoustic information since it measures particle velocity – a vector quantity. Nehorai and Paldi (1994) showed on a model basis that for this reason the AVS can outperform the scalar-sensor arrays in terms of accuracy for sound source localization. Moreover, the AVS allows the use of smaller array apertures such as the 3D Sound Intensity Probe, whilst maintaining performance.

Jing et al. (2014) studied the Delay-And-Sum (DAS) beamformer and Minimum-Variance-Beamforming (MVB) for pressure sensor arrays and a single AVS. Comparisons of simulations show the main advantages of the AVS over traditional microphone phased array systems: the frequency independent spatial resolution, the absence of ghost sources and the lack of spatial aliasing. On the other hand, the maximum number of sound sources and the dynamic range of the beamforming results are often more limited when using a single AVS. The following section describes the covariance matrix, steering vectors and beamforming algorithms used in the research discussed in this paper as stated by Jing et al.

2.1 Signal and covariance matrix of an AVS

For an AVS comprising one pressure microphone and three orthogonal particle velocity sensors, the signal matrix can be expressed as

$$y_v(\omega) = [p(x,\omega), u_x(x,\omega), u_y(x,\omega), u_z(x,\omega)]^T \tag{1}$$

The covariance matrix for this AVS is given by

$$\boldsymbol{R}_v = [y_v {y_v}^H] = \begin{bmatrix} pp^* & pu_x^* & pu_y^* & pu_z^* \\ u_x p^* & u_x u_x^* & u_x u_y^* & u_x u_z^* \\ u_y p^* & u_y u_x^* & u_y u_y^* & u_y u_z^* \\ u_z p^* & u_z u_x^* & u_z u_y^* & u_z u_z^* \end{bmatrix} \tag{2}$$

2.2 Steering vector of an AVS

A steering vector a can be expressed as

$$a(\theta, \varphi, \omega) = e^{j\omega\tau} \tag{3}$$

and is related to the angle of azimuth θ and elevation ϕ of the propagating wave fronts. For an AVS, the steering vector is weighted due to the directivity of the sensor elements, see Figure 2. With r_m being the sensor position projected in three orthogonal components of a Cartesian axis.

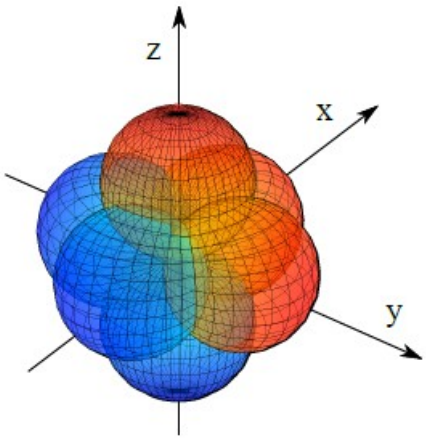

Figure 2: Directivity of an AVS.

The combination of the plane wave model and the directivity of the steering vector can be described for each sensor as follows:

$$w_p = e^{j\omega \frac{\cos(\varphi)\cos(\theta)r_x + \cos(\varphi)\sin(\theta)r_y + \sin(\varphi)r_z}{c}}$$

$$w_x = \cos(\varphi)\cos(\theta)w_p \tag{4}$$

$$w_y = \cos(\varphi)\sin(\theta)w_p$$

$$w_z = \sin(\varphi)\, w_p$$

Resulting in the steering vector of an AVS:

$$a(\theta, \varphi, \omega) = [w_p, w_x, w_y, w_z]^T \tag{5}$$

2.3 Source localization with an AVS

The localization of noise sources is achieved by estimating the Direction of Arrival (DOA) of propagating wave fronts. In this paper the results of source localization through acoustic sound intensity mapping and beamforming are given.

Using acoustic sound intensity mapping, it is common to study acoustic sound fields in terms of the active, or propagating, part of the complex intensity (Fernández Comesaña, 2014). Time averaging, indicated by $< . >_t$ is applied. The imaginary part, also known as the reactive intensity, representing the non-propagating acoustic energy, is rejected.

$$I = \{I_x, I_y, I_z\} = < pu >_t = \frac{1}{2} Re\{pu\} \tag{6}$$

For beamforming, the geometry information of the AVS is used in combination with the processed signals, recorded by each sensor to create spatially discriminating filters. The Delay-And-Sum (DAS) beamformer and Minimum-Variance-Beamforming (MVB) spectra are

$$P_{DAS}(\theta, \varphi, \omega) = \boldsymbol{a}^{\boldsymbol{H}}(\theta, \varphi, \omega)\boldsymbol{R}(\omega)\boldsymbol{a}(\theta, \varphi, \omega) \tag{7}$$

$$P_{MVB}(\theta, \varphi, \omega) = [\boldsymbol{a}^{\boldsymbol{H}}(\theta, \varphi, \omega)\boldsymbol{R}^{-\boldsymbol{1}}(\omega)\boldsymbol{a}(\theta, \varphi, \omega)]^{-\boldsymbol{1}} \tag{8}$$

3. Experimental evaluation

The aim of this section is to investigate the sound field produced by a complex structure – a wind turbine – and to localize noise sources for a particular frequency band FBx. This includes measurements on the outside of the full wind turbine, covering the tower, nacelle and blades.

3.1 Measurement set up

The measurement set up comprises a standard laptop, one Microflown 3D Sound Intensity Probe, a signal conditioner, data acquisitioning system and a USB-webcam (Figure 3, left). Sound pressure and three channels of particle velocity are recorded at a sampling frequency of 48 kHz. Video image of the wind turbine is recorded at 10 f/s and may be used in further research to plot the results according to different blade positions. It is not used for the results described in this paper. The length of each recording is 5 minutes and the set-up time is 2 minutes. Measurements are done at tower-sensor distances of 50 m and 100 m to investigate environmental influences and ground reflections.

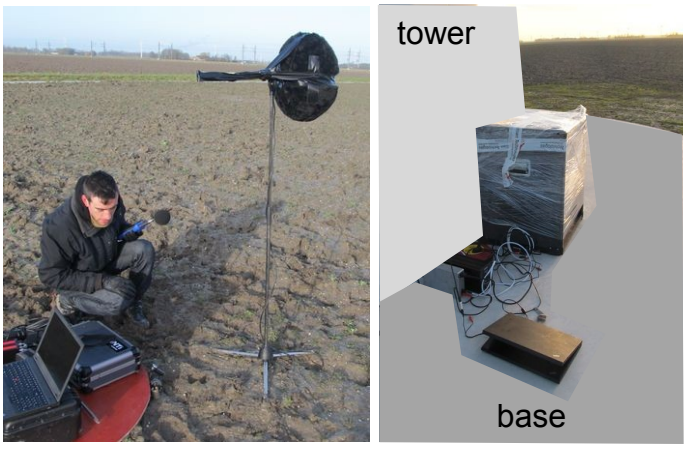

Figure 3: Measurement setup (left) and loudspeaker functioning as reference acoustic source (right).

A loudspeaker positioned at the base of the wind turbine tower functions as a reference acoustic source (Figure 3, right). The reference signal consists of three sinusoidal tones of 60 Hz, 200 Hz and 250 Hz.

3.2 Wind cap

Two different wind caps were tested, a spherical and a cylindrical shaped wind cap. Results show that both prototypes enable the measurement of particle velocity near to a wind turbine. However, only the spherical wind cap provides consistent estimation of elevation. Therefore, all DOA results presented in this paper were calculated using the data acquired with the spherical wind cap.

Figure 4: Spherical (left) and cylindrical (right) wind caps.

4. Results

In the spectra of the recorded signals, FBx excited by the wind turbine is present. The three reference tones 60Hz, 200Hz and 250Hz are clearly visible. 150s of the acoustic data was processed in time blocks of 4s using a FFT size of 9600 and a Hanning window. To filter the reference tones, a 5th order Butterworth band-pass filter was applied in the time domain with a bandwidth of 10 Hz.

4.1 DOA using Acoustic Intensity

The results in Figure 5 show that the reference sound source is accurately detected using any of the tones. The consistent location of the three frequencies proves the reliability of the reference signal. The figure shows results for both 50m (top and bottom-left) and 100m (bottom-right) tower-sensor distances. Apparently the net intensities received at the two measurement positions have different sources. However, it seems that the 50m measurement perceives the sum of the real source and the ground reflection as the origin. Beamforming algorithms are applied in the following sections to avoid this problem.

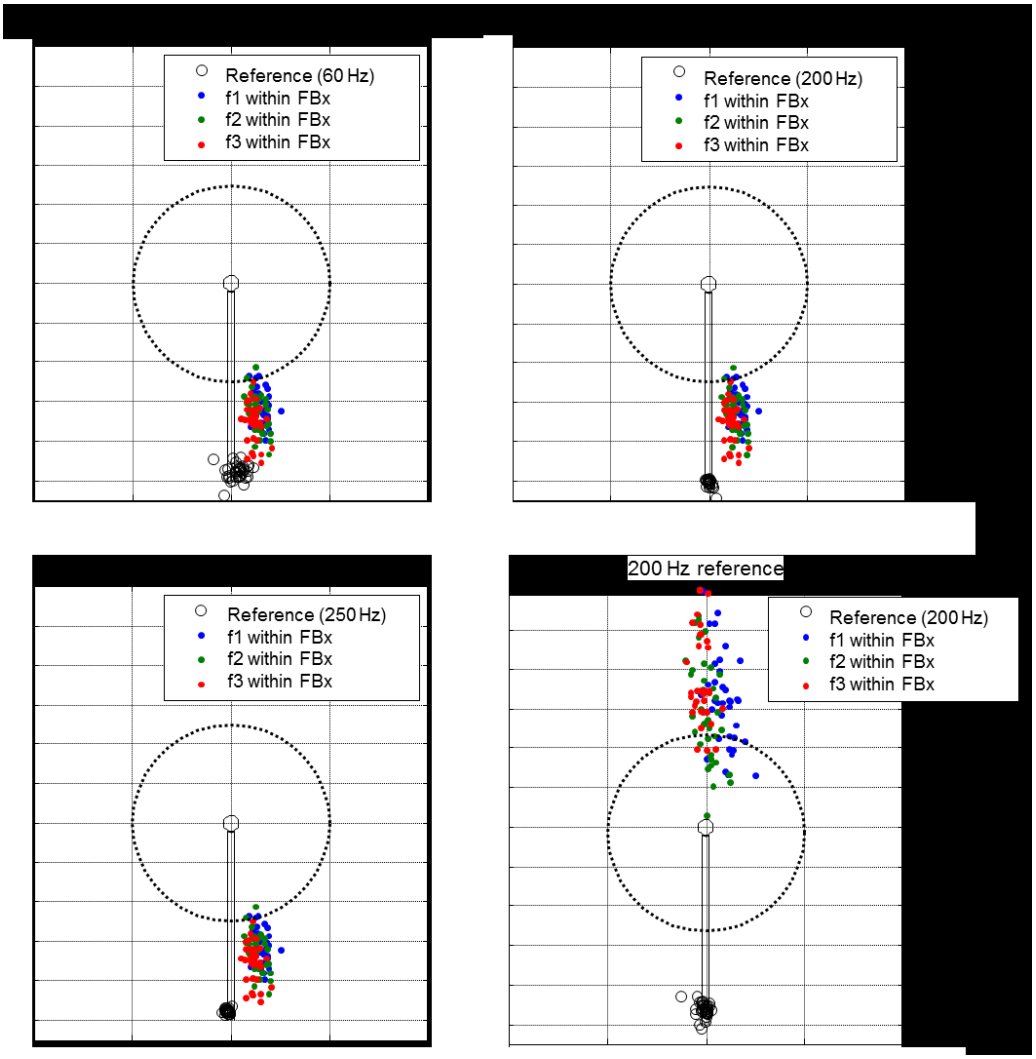

Figure 5: DOA using acoustic intensity mapping for different reference tones (60 Hz, 200 Hz, 250 Hz) measured at 50 m and with 200 Hz reference tone measured at 100 m (bottom-right).

4.2 DOA using DAS beamforming

Conventional Delay-And-Sum beamforming (DAS) is able to locate the reference loudspeaker in both positions. However, the source of FBx appears to change position if the measurement is performed at a distance of 50m or 100m from the wind turbine. The results in Figure 6 are similar to the intensity analysis. The colored dynamic range is 2 dB. One of the main limitations of both methods is that they cannot distinguish multiple correlated sources.

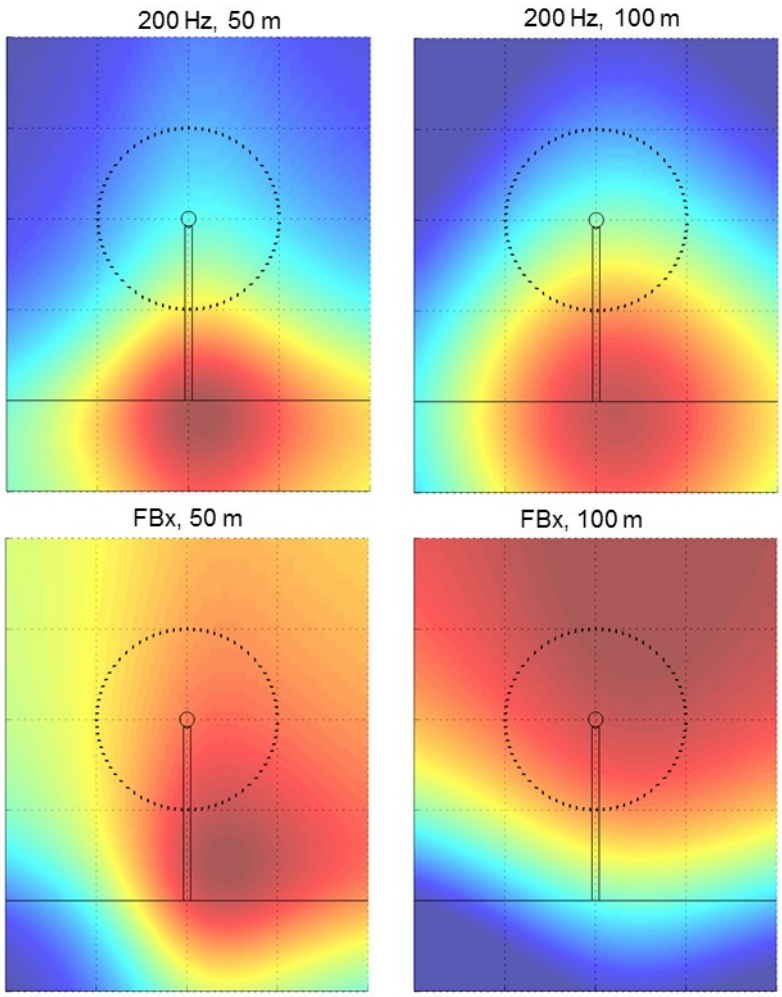

Figure 6: DOA using DAS beamforming for the reference source of 200 Hz (top row) and FBx (bottom row) measured at 50m (left column) and 100m (right column) tower-sensor distance.

4.3 DOA using MVB

Minimum-Variance-Beamforming (MVB) is implemented to improve the performance of the DOA. MVB is able to distinguish between the real source and its ground reflection even at 50m, highlighted with a white circle in the bottom-right image of Figure 7. The slight deviation that can be seen at 60 Hz reference may also affect the band of interest. In such a case, the whole map should be moved. The results of DOA using MVB are given in Figure 7 for measurements at 50m tower-sensor distance and Figure 8 for 100m. The colored dynamic range is 10 dB. The MVB results are consistent for both distances.

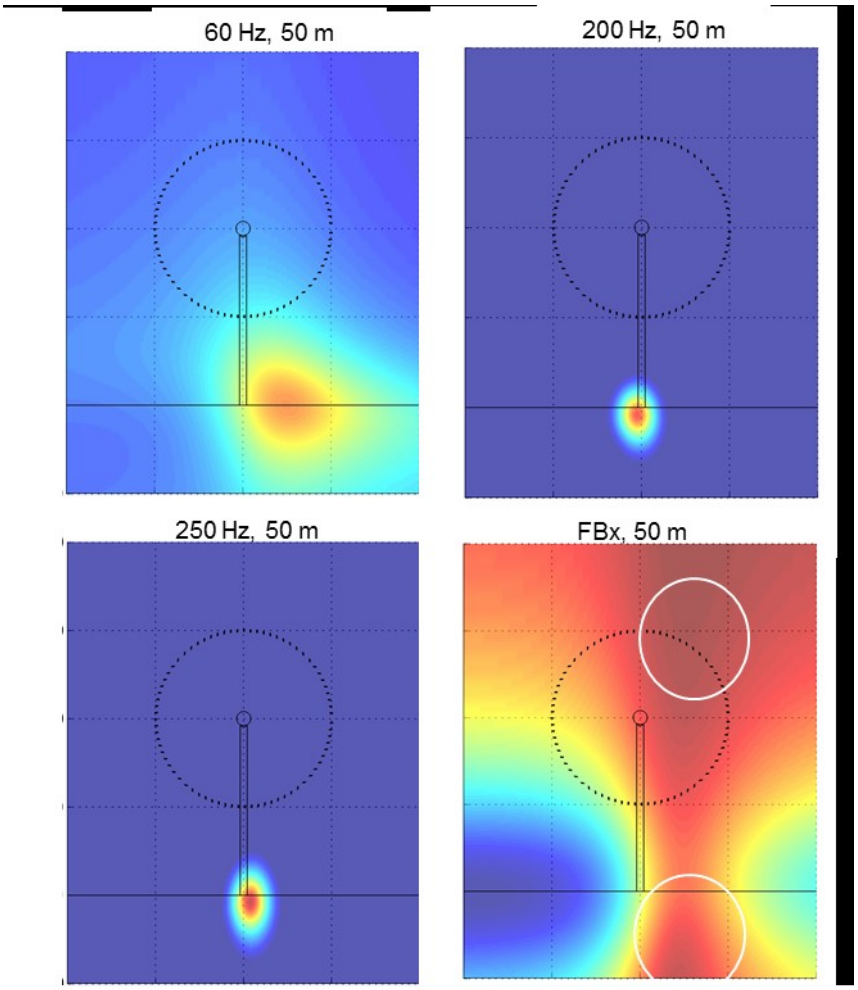

Figure 7: Results of DOA using MVB measured at 50 m tower-sensor distance.

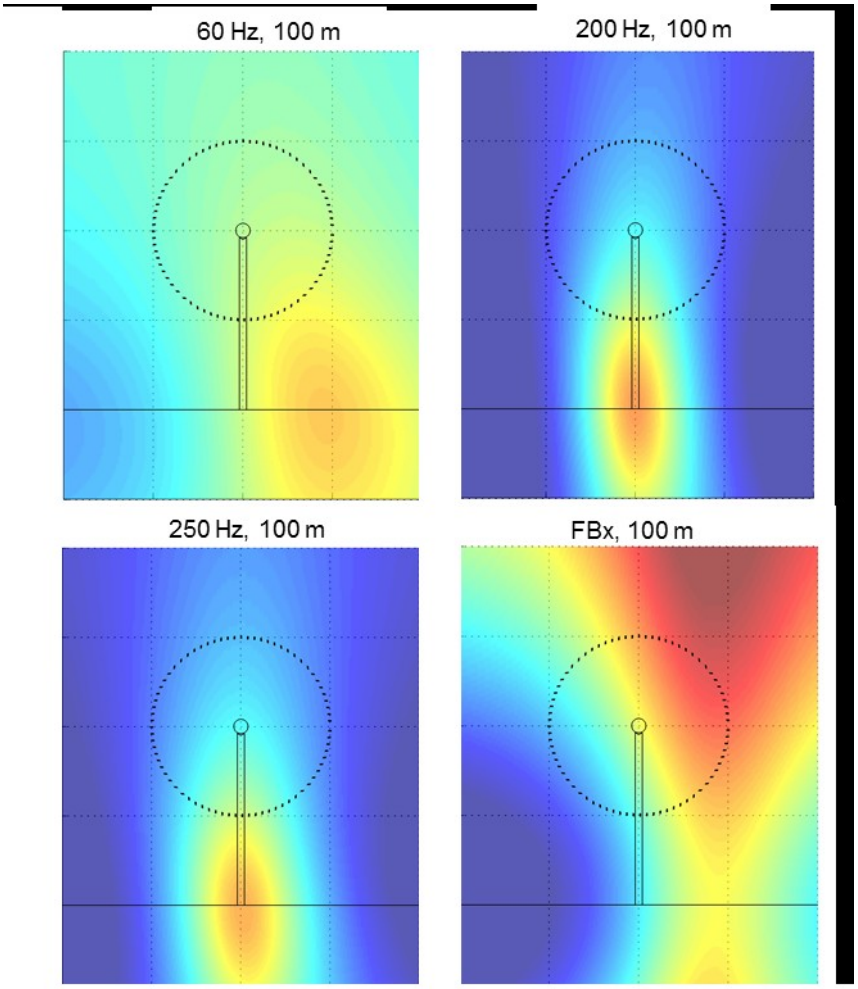

Figure 8: Results of DOA using MVB measured at 100 m tower-sensor distance.

5. Conclusions

Outdoor measurements in a wind turbine park are now possible using an AVS with a large wind cap. Experimental tests show that cylindrical wind caps enable stable azimuth estimation. But spherical wind caps are required to also get a consistent estimation of the source elevation.

The results show that an AVS can be used for sound source within the 50 – 250 Hz frequency range on a multi-megawatt wind turbine. 3D sound intensity can be used as an estimation of the DOA as long as the ground reflection is not too strong. Advance beamforming algorithms like MVB can avoid the issue of ground reflection with the ability to distinguish between two coherent sound sources. The noise source of FBx is identified to be at the top-center of the blades, assuming that the plotted source is shifted to the right as is the 60 Hz reference source.

Further processing of the measurements along with the recorded video image can be done to locate noise sources in relation to different blade positions. The results presented in this paper are time averaged over all blade positions. Additional measurements at the side of the turbine may enable triangulating the real position of the source in a three dimensional space. More measurements and research are

required to provide more accurate sound source localization and define solid conclusions.

6. Discussion

Ground reflections are more apparent for measurements done at 50m compared to the 100m measurements. It is assumed that this is caused by the change in ground impedance, depending on the sound angle of incidence and the ground materials, which is different for the two positions. It is not clear which one contributes more to the change in impedance.

References

Basten T. et al. (2009). *Multiple incoherent sound source localization using a single vector sensor.* ICSV16, Krakow, Poland.

Fernández Comesaña D. (2014). *Scan-based sound visualization methods using sound pressure and particle velocity.* University of Southampton, United Kingdom.

Hawkes M. and Nehorai A. (1998). *Acoustic Vector-Sensor Beamforming and Capon Direction Estimation.* IEEE Transactions on signal processing, Vol. 46, No. 9.

Jing W.Q. et al. (2014). *Sound source localisation using a single acoustic vector sensor and multichannel microphone phased arrays.* Internoise 2014, Melbourne, Australia.

Nehorai A. and Paldi E. (1994). *Acoustic Vector-sensor array processing.* Signal processing, IEEE Transactions on. 1994;42(9):2481-2491.

Oerlemans, S. (2009). *Detection of aeroacoustic sound sources on aircraft and wind turbines PhD thesis.* University of Twente, The Netherlands.

Raangs R. and Druyvesteyn E. (2002). *Sound Source Localization Using Sound Intensity Measured by a Three Dimensional PU-probe.* Audio Engineering Society Convention 112.

Wind J. et al. (2009). *Acoustic vector sensors for aeroacoustics.* CEAS.

Wind J. and de Bree H.E. (2010). *3D sound source localization and sound mapping using a p-u sensor array.* Proceedings of CAES-AIAA.